Pore Formation and Translocation of Melittin

Katsumi Matsuzaki, Shuji Yoneyama, and Koichiro Miyajima
Faculty of Pharmaceutical Sciences, Kyoto University, Sakyo-ku, Kyoto 606-01, Japan

ABSTRACT Melittin, a bee venom, is a basic amphiphilic peptide, which mainly acts on the lipid matrix of membranes, lysing various cells. To elucidate the molecular mechanism, we investigated its interactions with phospholipid vesicles. The peptide formed a pore with a short lifetime in the membrane, as revealed by the release of an anionic fluorescent dye, calcein, from the liposomes. Our new double-labeling method clarified that the pore size increased with the peptide-to-lipid ratio. Upon the disintegration of the pore, a fraction of the peptides translocated across the bilayer. The pore formation was coupled with the translocation, which was proved by three fluorescence experiments recently developed by our laboratory. A novel model for the melittin pore formation was discussed in comparison with other pore-forming peptides.

INTRODUCTION

Melittin (H_2N-Gly-Ile-Gly-Ala-Val-Leu-Lys-Val-Leu-Thr-Thr-Gly-Leu-Pro-Ala-Leu-Ile-Ser-Trp-Ile-Lys-Arg-Lys-Arg-Gln-Gln-$CONH_2$), a basic (+6) hexacosa peptide, is a major protein component of the European honey bee *Apis mellifera* (for recent reviews, see Cornut et al., 1993; Dempsey, 1990; Saberwal and Nagaraj, 1994; Sansom, 1991). The peptide is well known for its strong hemolytic potency, but it also kills other eukaryotic and prokaryotic cells (Steiner et al., 1981). These activities have been mainly discussed in terms of its interactions with the lipid matrix of biomembranes, although the involvement of membrane proteins (Clague and Cherry, 1989; Dufton et al., 1984) was additionally suggested. There is a consensus that a peptide-induced loss of membrane barrier property is primarily responsible for the cytolytic activity. Melittin causes the efflux of water-soluble fluorescent markers entrapped within liposomes at lower peptide-to-lipid ratios (P/L), which depend on the lipid composition and the osmotic gradient across the membrane (Benachir and Lafleur, 1995, 1996). At higher peptide contents, it micellizes the vesicles (Dufourcq et al., 1986). The peptide also forms voltage-gated ion channels in planar lipid bilayers (Pawlak et al., 1991; Stankowski et al., 1991; Tosteson et al., 1990).

Lipid bilayers are an excellent model system for investigating the underlying molecular mechanism by use of various spectroscopic and thermal techniques. Despite extensive studies, however, the details are still in chaos. Melittin in membranes forms an amphiphilic α-helix with a flexible hinge around Pro^{14} and an unordered C-terminal at the 22–26 residues (Okada et al., 1994). Its orientation with respect to the bilayer surface can be parallel, perpendicular, or even random, depending on the lipid used and the extent of hydration (Frey and Tamm, 1991; Vogel, 1987). Melittin oligomers appear to be involved in membrane permeabilization, which supralinearly depends on the peptide concentration in both voltage-gated ion channel experiments (Pawlak et al., 1991; Stankowski et al., 1991; Tosteson et al., 1990) and a dye release study in the absence of the transmembrane potential (Schwarz et al., 1992; Stankowski et al., 1991). On the contrary, researchers failed to detect significant interpeptide aggregation (Altenbach and Hubbell, 1988; Hermetter and Lakowicz, 1986; John and Jänig, 1991; Schwarz and Beschiaschvili, 1989). An explanation for this apparent discrepancy could be that only a minor fraction of the peptide forms the membrane-spanning pore. Another interpretation is that monomeric melittin can disturb the lipid organization at the membrane-water interface, leading to enhanced membrane permeability ("wedge effect"; Terwilliger et al., 1982), and the application of the potential switches the orientation of the helix from parallel to perpendicular to the membrane surface, promoting peptide aggregation. It is also controversial whether the ion channel observed only under the influence of the trans-negative potential can be equated with the pore in the absence of the electric field.

In this study we focused on the mechanism of melittin pore formation in liposomal membranes in the absence of the transmembrane potential. This system could be a model of hemolysis because the transmembrane potential across the erythrocyte membrane is negligibly small (Rink and Hladky, 1982). We have determined that other pore-forming peptides, magainin 2 (Matsuzaki et al., 1995a,b) and mastoparan X (Matsuzaki et al., 1996b), translocate across the bilayer by forming a pore. It is significantly important in understanding the basic principles of peptide-lipid interactions to clarify whether peptides of different charges, sizes, hydrophobicities, and lipid specificities behave alike.

In the first part of this paper, the translocation of synthetic melittin was detected by three methods. The pore formation was then determined on the basis of the efflux of an anionic fluorescent dye, calcein, from large unilamellar vesicles (LUVs). The pore formation was coupled with the translocation. The lifetime of the pore was estimated to be rather

Received for publication 25 September 1996 and in final form 12 May 1997.

Address reprint requests to Dr. Katsumi Matsuzaki, Faculty of Pharmaceutical Sciences, Kyoto University, Sakyo-ku, Kyoto 606-01, Japan. Tel.: 81-75-753-4574; Fax: 81-75-761-2698; E-mail: katsumim@pharm.kyoto-u.ac.jp.

0006-3495/97/08/831/08 $2.00

short, based on the self-quenching property of this fluorophore. Furthermore, to evaluate the dependence of the pore size on the P/L, we developed a new "double-labeling" technique, in which both the aqueous and membranous phases are labeled with fluorescent probes. We found that the pore size increases with the P/L. The pore formation mechanism was discussed on the basis of these findings.

MATERIALS AND METHODS

Materials

Synthetic melittin (Bachem, Budendorf, Switzerland) was used to avoid the contamination of phospholipase A_2 and the formylated peptide. The manufacturer had checked the purity by high-performance liquid chromatography (>98%) and amino acid analysis. The concentration of a peptide stock solution was routinely determined by optical density at 280 nm. Egg yolk L-α-phosphatidylcholine (egg PC) and fluorescein isothiocyanate-dextran of MW 4400 (FITC-dextran) were purchased from Sigma (St. Louis, MO). L-α-Phosphatidyl-DL-glycerol (egg PG) enzymatically converted from egg PC was a kind gift from Nippon Fine Chemical Co. (Takasago, Japan). *N*-[[5-(Dimethylamino)naphthyl]-1-sulfonyl]dipalmitoyl-L-α-phosphatidylethanolamine (DNS-PE) and *N*-(7-nitrobenz-2-oxa-1,3-diazol-4-yl)dipalmitoyl-L-α-phosphatidylethanolamine (NBD-PE) were products of Molecular Probes (Eugene, OR). Calcein and spectrograde organic solvents were supplied by Dojindo (Kumamoto, Japan). All other chemicals (from Wako, Tokyo, Japan) were of special grade. A Tris-HCl buffer (10 mM Tris/150 mM NaCl/1 mM EDTA, pH 7.0) was prepared from water distilled twice in a glass still.

Vesicle preparation

LUVs were prepared by extrusion of MLVs, as described elsewhere (Matsuzaki et al., 1994). Briefly, a lipid film, after being dried under vacuum overnight, was hydrated with a 70 mM calcein solution for the dye release assay (pH was adjusted to 7.0 with NaOH) or the Tris buffer for the other experiments and vortex-mixed to produce MLVs. The suspension was freeze-thawed for five cycles and then successively extruded through polycarbonate filters (a 0.6-μm pore size filter, five times; two stacked 0.1-μm pore size filters, 10 times). The lipid concentration was determined in triplicate by phosphorus analysis (Bartlett, 1959).

Calcein leakage

The calcein-entrapped LUVs were separated from free calcein on a Biogel A 1.5-m column. The release of calcein from LUVs was fluorometrically monitored at an excitation wavelength of 490 nm and an emission wavelength of 520 nm on a Shimadzu RF-5000 spectrofluorometer, the cuvette holder of which was thermostated at 30 ± 0.5°C. The maximum fluorescence intensity, corresponding to 100% leakage, was determined by the addition of 10% Triton X-100 (20 μl) to 2 ml of the sample. The mode of leakage was examined, as described earlier (Matsuzaki et al., 1994, 1997; also see text).

FITC-dextran leakage

A double-labeling method was developed. LUVs of egg PC/egg PG/DNS-PE (9:0.85:0.15) trapped with 3 mM FITC-dextran (MW 4400) were incubated with the peptide. A large excess of unlabeled LUVs (egg PC/egg PG = 9:1) was added to stop the membrane permeabilization. The leaked FITC-dextran was removed by gel filtration (Bio-Gel, A-15 m). The excitation spectrum of the vesicle fraction after solubilization with Triton X-100 was measured at an emission wavelength of 520 nm.

Resonance energy transfer

Symmetrically labeled LUVs were prepared by hydrating the lipid film composed of either egg PC/DNS-PE (9:1) or egg PC/egg PG/DNS-PE (9:0.5:0.5). Resonance energy transfer (RET) from the Trp residue of the peptide to the dansyl chromophore in the membrane was monitored by observing the fluorescence intensity of either the Trp residue (336 nm) or the dansyl group (510 nm) upon excitation at 280 nm or 285 nm, respectively. The temperature was controlled at 30 ± 0.5°C.

Dithionite ion permeability

A lipid film composed of egg PC/egg PG/NBD-PE (9:1:0.025, mol/mol) was hydrated with the buffer and vortex-mixed. The suspension was freeze-thawed for five cycles. Small aliquots of the MLVs were injected into a buffer (control) or a melittin solution in the presence of 10 mM sodium dithionite. The fluorescence intensity of NBD at 530 nm (excited at 450 nm) was monitored at 30°C. The intensity was represented relative to the value in the absence of the reducing ion.

RESULTS

Translocation

The translocation of melittin across lipid bilayers was detected by the use of two methods. The first technique measures the amount of the untranslocated peptides remaining in the outer monolayers (Matsuzaki et al., 1995a). The untranslocated peptides can be readily removed from the vesicle surface by extraction with a large excess of a second population of vesicles. The unremovable fraction was determined by use of RET from the Trp residue of melittin to the dansyl chromophore (DNS-PE) incorporated into the membrane phase.

Fig. 1 shows that the addition of dansyl-labeled LUVs (egg PC/DNS-PE, 9:1) to a peptide solution at time 0 (P/L = 0.0075) resulted in a significant decrease in Trp fluorescence, indicating RET due to the binding of the peptide to the membrane. After a short incubation for 0.5 min, a second population of dansyl-free vesicles (DNS-PE was substituted by egg PG) was added in large excess (*trace 2*). An increase in the fluorescence intensity implies that the peptide molecules, which had been bound to the outer leaflet, were redistributed between the two vesicle populations, resulting in relief from RET. The increased fluorescence intensity, however, was smaller than the intensity when both populations of vesicles were added simultaneously to the peptide solution at time 0 (*trace 1*), suggesting that a fraction of the peptides became unexposed to the outer surface and therefore untransferable to the second vesicles. The buried fraction increased with the incubation time (*traces 2–5*), indicating a time-dependent translocation of the peptide.

It should be here noted that the peptide might translocate via the aqueous pore if a significant fraction of the peptide existed as the free form. However, this possibility can be rejected for the following reasons. First, the fluorescence intensity in the presence of the dansyl LUVs (Fig. 1, *lower traces*) was almost constant with respect to time, indicating that the number of membrane-bound peptide molecules did

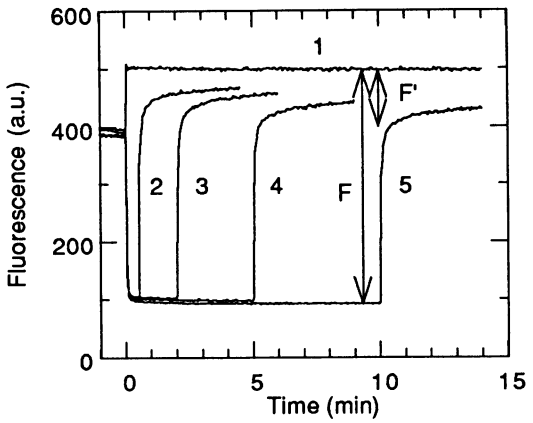

FIGURE 1 Detection of the peptide translocation. Melittin was mixed with dansyl-LUVs (egg PC/DNS-PE = 9:1) at time 0. The final peptide and lipid concentrations were 2 and 265 μM, respectively. The fluorescence intensity of Trp at 336 nm (excited at 280 nm) was recorded. The binding of the peptide to the vesicle reduced the intensity because of RET. At various time intervals of incubation (0.5, 2, 5, 10 min, *traces 2–5*), a large excess (final concentration ~1 mM) of the second population of dansyl-free LUVs (egg PC/egg PG = 9:1) was added. An increase in intensity indicates the relief from RET caused by the redistribution between the two vesicle populations of the peptide molecules that had been bound to the outer surface of the first vesicle. The increased intensity decreases with prolonged incubation and is smaller than the fluorescence intensity when both populations of vesicles were simultaneously added at time 0 (*trace 1*), thus indicating that some of the peptides translocated into the inner leaflet during the incubation. Each trace is the average of three experiments.

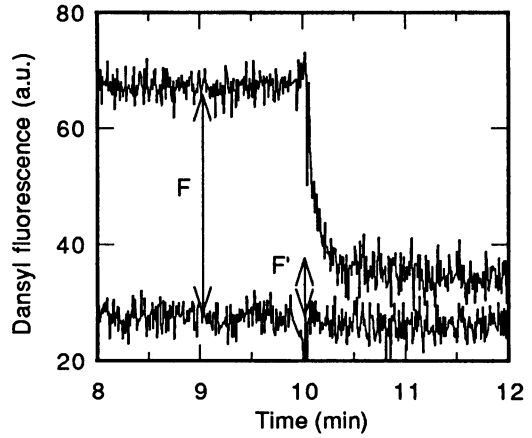

FIGURE 2 Detection of the peptide translocation. Melittin was mixed with dansyl-LUVs (egg PC/egg PG/DNS-PE = 9:0.5:0.5) at time 0. The final peptide and lipid concentrations were 2 and 569 μM, respectively. The sensitized fluorescence of dansyl at 510 nm (excited at 285 nm) was recorded. The binding of the peptide to the vesicle enhanced the intensity because of RET. After 10 min (*upper trace*), a large excess (final concentration ~2.5 mM) of the second population of dansyl-free LUVs (egg PC/egg PG = 9:1) was added. An decrease in intensity indicates the relief from RET caused by the redistribution between the two vesicle populations of the peptide molecules that had been bound to the outer surface of the first vesicle. The decreased intensity is larger than that of the lower trace where both populations of vesicles were simultaneously added at time 0, indicating that some of the peptides translocated into the inner leaflet during the incubation. Each trace is the average of three experiments.

not change during the incubation. If there had been a large fraction of free melittin, the amount of bound peptide should have largely increased upon translocation, because the inner leaflets also should have become available for the peptide as a binding site. Second, further addition of the dansyl vesicles did not change the fluorescence intensity further (data not shown), suggesting that the free fraction was negligible.

The translocation at a lower P/L value of 0.0035 was detected by measuring the sensitized dansyl fluorescence, because a large light scattering after the addition of a second population of dansyl-free liposomes hampered the precise determination of the Trp fluorescence. A melittin solution (2 μM) was incubated with dansyl LUVs (569 μM) for 10 min. The dansyl fluorescence intensity at 510 nm was monitored upon excitation at 285 nm. A large contribution from direct excitation was corrected by subtracting the intensity in the absence of the peptide. In this experiment, the fraction of DNS-PE was reduced to 5 mol% to more effectively extract the sensitized fluorescence from the intense background signal. The upper trace in Fig. 2 shows that the addition of a large excess of dansyl-free vesicles at 10 min (final concentration 2.5 mM) abruptly decreased the sensitized fluorescence because of relief from RET. The reduced intensity was, however, larger than the value of the lower trace, where the two populations of the LUVs were co-added at time 0, suggesting that a fraction of the peptide translocates into the inner monolayers, and therefore is untransferable to the dansyl-free liposomes.

To compare the two methods, the translocation of melittin at the higher P/L value (0.0075) was also estimated with the latter technique. The two approaches gave similar results (cf. *open and closed circles* in Fig. 4).

Fig. 3 more directly proves the peptide translocation. The

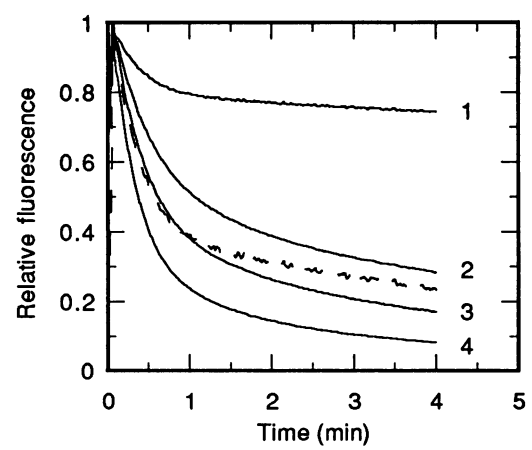

FIGURE 3 Detection of the peptide translocation. Small aliquots of MLVs composed of egg PC/egg PG/NBD-PE (9:1:0.025) were injected into a buffer (*curve 1*) or a melittin solution (*curves 2–4*) in the presence of 10 mM sodium dithionite. The essentially membrane-impermeable ion chemically quenches the NBD fluorescence. The fluorescence at 530 nm (excitation at 450 nm) was normalized to the intensity in the absence of the reducing ion. The peptide concentrations of curves 2, 3, and 4 were 0.25, 0.5, and 1 μM, respectively. [lipid] = 99 μM. The dashed trace is the calculated curve in the case of no translocation.

addition of sodium dithionite to MLVs doped with NBD-PE reduced the chromophores exposed to the external aqueous phase, making them nonfluorescent (*trace 1*). The fluorescence decrease, corresponding to the fraction of the NBD groups on the vesicular surface, was 25%, indicating that the lamellarity of the vesicle is 2 or larger: the anionic bilayers tend to swell because of electrostatic repulsion, and the circumference of each lamella grows significantly as one moves away from the center. If the peptide permeabilizes only the outermost bilayers (i.e., no translocation), the reagent can react with the chromophores facing the first interlamellar space, resulting in quenching of less than 75%. The expected time course of quenching in this case is shown as the dashed curve in Fig. 3, assuming that the dithionite concentration in the first interbilayer space is instantaneously equilibrated with that in the external aqueous phase. The addition of melittin at a P/L value of 0.0025 (*trace 2*) permeabilized only the outermost bilayers. In contrast, at higher P/L values of 0.005 (*trace 3*) and 0.01 (*trace 4*), the quenching curves lay below the dashed curve; the peptide molecules translocated across the outermost bilayers to form pores in the inner bilayers.

Coupling between pore formation and translocation

The pore formation of melittin was assayed on the basis of the efflux of an anionic, fluorescent dye, calcein, from LUVs composed of egg PC/egg PG (9:1) under the same conditions as in Figs. 1 and 2. According to Schwarz's theory (Schwarz and Robert, 1992; Schwarz and Arbuzova, 1995), the number of pores per vesicle (p) that had been formed from $t = 0$ to t can be expressed by

$$p = -(\ln R)/(1 - \rho) \quad (1)$$

The retention of the dye was denoted by R ($0 \leq R \leq 1$). A dimensionless parameter, ρ, describes the pore life span:

$$\rho = \tau_0/(\tau + \tau_0) \quad (2)$$

τ and τ_0 are the pore lifetime and the intrinsic lifetime, respectively. The latter is the time necessary for a $1/e$ reduction of the intravesicular dye concentration and is estimated to be ~10 ms (Matsuzaki et al., 1995b). If τ is much longer than τ_0, a single pore opening is sufficient to exhaust the vesicular contents ("all-or-none mode," $\rho \rightarrow 0$). On the other hand, a number of pore openings are necessary to observe a significant extent of leakage in the case of $\tau \ll \tau_0$ ("graded mode," $\rho \rightarrow 1$). There are, of course, many cases between the above two extremes. The ρ value can be evaluated by determination of the percentage self-quenching value of the intravesicular dye after the peptide treatment. After the calcein-containing egg PC/egg PG (9:1) LUVs were mixed with the peptide at 30°C ([peptide] = 1 μM, [lipid] = 152 μM), the time course of the calcein fluorescence increase was monitored in a cuvette for 10 min. Aliquots of the liposome suspension were immediately added to an Eppendorf tube containing a fivefold excess of calcein-free LUVs to stop the leakage. Triton X-100 was added to the cuvette to completely lyse the vesicles. The apparent retention, E, was calculated according to

$$E = (F_t - F)/(F_t - F_0) \quad (3)$$

F and F_t denote the fluorescence intensity before and after the detergent addition, respectively. F_0 represents the fluorescence of the intact vesicle. The E value was 0.301. On the other hand, the liposomes in the Eppedorf tube were applied on a Bio-Gel A 1.5-m column. The vesicle fraction was separated from the leaked calcein by gel filtration, and its quenching factor (Q) was obtained by measuring the fluorescence intensity before (F_b) and after (F_a) the addition of Triton X-100:

$$Q = F_b/F_a \quad (4)$$

The observed value was 0.397 ± 0.027. The predicted Q values for $\rho = 1$ and $\rho = 0.95$ are 0.391 and 0.382, respectively. Therefore, we conclude that melittin forms a short-lived pore ($\rho \approx 1$). The details of the calculation have been described elsewhere (Schwarz and Arbuzova, 1995).

Fig. 4 compares the translocation with the pore formation. The extent of translocation was estimated by F'/F in Fig. 1 (*closed circles*) or in Fig. 2 (*open symbols*). F' was obtained by linear extrapolation of the slower phase of the fluorescence change due to "back-translocation" to the time of addition of the dansyl-free liposomes. The F'/F value was converted to r_i, the amount of the translocated peptide per lipid (Matsuzaki et al., 1995b, 1996b). The pore formation was expressed by $-\ln R$, which is proprtional to p (Eq. 1). The observed E value was transformed to R, assuming $\rho = 1$ (Schwarz and Arbuzova, 1995). A linear relation was observed between r_i and $-\ln R$, indicating that the amount

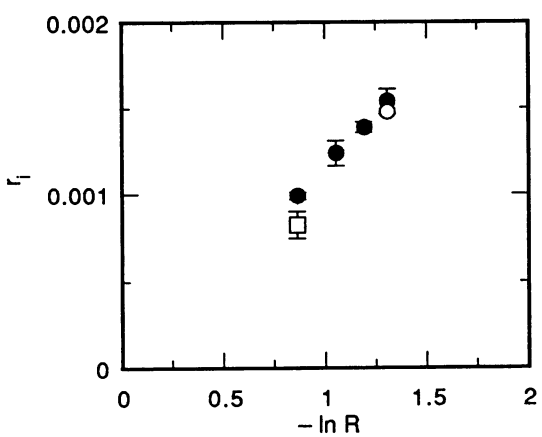

FIGURE 4 Relationship between pore formation and peptide translocation. The pore formation was estimated on the basis of the leakage of calcein from egg PC/egg PG (9:1) LUVs and expressed by $-\ln R$ (R, retention). The translocation was evaluated by the F'/F values in Figs. 1 (●) and 2 (○), and is converted to r_i, the amount of the translocated peptide per lipid. P/L values were 0.0035 (□) and 0.0075 (○, ●). Results from three experiments are plotted.

of the translocated peptide is proportional to the number of the pores formed. Under the conditions in Fig. 4, 100–200 melittin molecules per vesicle were internalized upon the disintegration of many short-lived pores ($\rho \approx 1$).

Dependence of pore size on *P/L*

The pore size can be a function of the P/L. We employed another larger solute, FITC-dextran 4400, as a water-soluble marker. To evaluate the extent of its leakage, we developed a double-labeling technique. Briefly, the membrane and the aqueous phases were labeled with DNS-PE and FITC-dextran, respectively. After incubation with the peptide for 5 min, excess dansyl-free LUVs were added to stop the leakage. The vesicle fraction was separated from the leaked dye by gel filtration (Bio-Gel A 15-m) and was solubilized with Triton X-100. The excitation spectra of the sample and the control without the peptide were measured at an emission wavelength of 520 nm. The spectra were normalized at 490 nm, where only FITC absorbs the light (Fig. 5). Trace 2 shows the spectrum of the control. A peak at 340 nm is due to DNS absorption. The extinction of FITC is rather small at this wavelength (*trace 1*). In the peptide-treated specimen (*trace 3*), the fluorescence intensity at 340 nm was higher compared with the value of the control (*trace 2*), indicating that the peptide-induced loss of entrapped FITC enhanced the contribution of the DNS-lipid fluorescence relative to the fluorescent polymer. The extent of leakage was calculated by $(F - F_0)/F$. An advantage of this novel method is that one must measure only the spectrum of the vesicular fraction, instead of determining the fluorescence intensity of all fractions.

Fig. 6 depicts the percent leakage values of calcein (*open circles*) and the fluorescent dextran (*closed circles*) as a function of P/L. The two solutes were released at different concentration ranges: the smaller dye leaked at P/L < 0.01, whereas the larger polymer started to permeate at P/L > 0.01, suggesting that the pore size depends on the P/L.

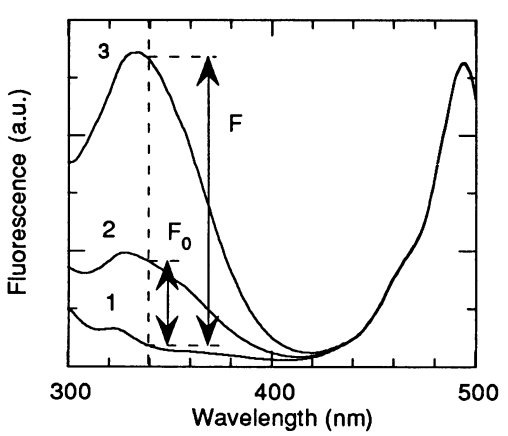

FIGURE 5 Determination of leakage of FITC-dextran by a double-labeling technique. The aqueous phase of egg PC/egg PG/DNS-PE (9:0.85:0.15) LUVs was labeled with 3 mM FITC-dextran (MW 4400). Traces 1–3 show the excitation spectra of an FITC dextran solution, the solubilized vesicles without the peptide, and the solubilized vesicle fraction with a 5-min peptide treatment ([peptide] = 4 μM. [lipid] = 174 μM). The emission wavelength was 520 nm. The spectra (the average of two experiments) are normalized at 490 nm. See the text for details.

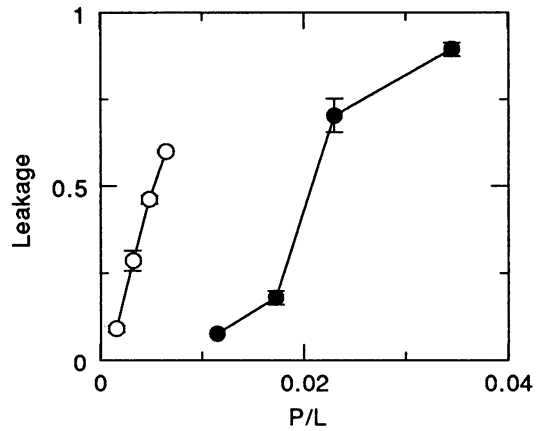

FIGURE 6 Dependence of pore size on P/L. The extent of leakage of calcein (○) and FITC-dextran (●) was plotted as a function of P/L. The data are the average of two to three experiments.

DISCUSSION

We revealed that melittin forms a short-lived pore, the size of which depends on the P/L (Fig. 6). Upon the disintegration of the pore, a fraction of the peptides translocates across the lipid bilayer (Figs. 1–3). The translocation is coupled with the pore formation (Fig. 4). It should be noted that vesicular fusion could result in an apparent translocation and a transient pore formation. We monitored the 90° light scattering intensity at 400 nm with the spectrofluorometer. The intensity increased by only 5%, even at a high P/L value of 0.026. This small enhancement can be explained by an expansion of the vesicular surface area and an increase in the refractive index. Therefore, we reject the possibility of fusion.

Translocation

A number of studies have reported on the mechanism of melittin pore formation. An important feature of the pore formation, which has often been overlooked, is the existence of the "pore deactivation process" (Schwarz et al., 1992); the rate of pore formation is initially fast, but is subsequently reduced to reach a plateau in minutes. In other words, the process is a relaxation toward an equilibrium.

Any proposed mechanism should be in accordance with the dynamics. Our pore formation-translocation scheme can satisfactorily explain the relaxation behavior: because of the cooperative nature of the interhelix aggregation (Pawlak et al., 1991; Schwarz et al., 1992; Stankowski et al., 1991; Tosteson et al., 1990), the rate of pore formation is significantly reduced after the redistribution of the peptides between the two leaflets. One would fail to detect the "active

form" if one were to determine the orientation and the aggregation of the peptide in the equilibrium state, where few pores would still exist.

Kempf et al. (1982) reported the possibility of the melittin translocation under the influence of a trans-negative potential. An ion channel experiment by the group of Schwarz (Pawlak et al., 1991) is also compatible with this: initially asymmetrical current-voltage curves become symmetrical as more and more current passes the bilayer. Our results clearly demonstrate that the translocation of melittin can occur, even in the absence of the transmembrane potential. The peptide internalization was also deduced on the basis of the kinetics of hemolysis (DeGrado et al., 1982).

It was reported (Benachir and Lafleur, 1995) that the affinity of melittin for lyzed vesicles is higher than that for intact vesicles. The translocation phenomenon can explain this observation: in the lysed vesicles, the peptides are redistributed between the two leaflets. Therefore, the binding capacity of the outer monolayer is larger than that of the intact vesicles where the peptides exclusively accumulate on the vesicle surface at a higher density.

Pore structure and lifetime

There seems to be no consensus on the definition of the "pore." Some researchers use the term to describe a channel of a defined structure, like the alamethicin channel model, composed of parallel helices (Fox and Richards, 1982). Others include in its meaning a peptide-involved structural defect in membranes through which ions permeate. We employ the latter, broader definition.

Pore formation is coupled with the translocation (Fig. 4), suggesting that the pore is an intermediate structure during the transbilayer transport of the peptide. It is energetically quite unfavorable for the positively charged side chains of melittin to be exposed to the bilayer's hydrophobic core of a low dielectric constant. Therefore, one can reasonably assume that the pore more or less resembles the putative ion channel of a helix bundle type, although several differences, such as the mutual orientation of the helices (parallel or antiparallel), may be present. A supralinear dependence of the pore formation rate on the peptide concentration implies the involvement of peptide aggregation. Schwarz et al. (1992) reported that the application of an inside-negative potential facilitates the dye release from liposomes. The potential should stabilize one of the membrane-spanning orientations of the helix via the electric field-helix macro dipole interactions and electrophoretically promote the internalization of the basic peptide.

The life span of the melittin pore in the absence of the potential was estimated, by use of the self-quenching property of calcein, to be rather short (<10 ms). Benachir and Lafleur (1995) recently found that the leakage of the same dye occurs in the all-or-none mode, regardless of the lipid composition. The differences in experimental conditions may be responsible for the discrepancy. The pH of their system was 9, whereas ours was 7. The concentrations of the peptide and the lipid they employed were much higher. They also suggested that the dye leakage is more likely to be related to cooperative membrane perturbations than to the formation of a well-defined pore, because a large number ($\sim$250) of melittin molecules per vesicle is needed to trigger the leakage. This observation can be understood by the remembering that the monomer-pore equilibrium lies far to the monomer side. It is also plausible that the perturbation of the outer monolayer caused by the monomer "squeezes out" the surface-lying peptide, facilitating the pore formation.

The pore size increases with the P/L (Fig. 6), in keeping with the helix bundle model (Sansom, 1991). We recently found that the size of the mastoparan X pore also depends on the P/L (Matsuzaki et al., 1997). The diameters of calcein (MW 623) and the dextran (MW 4400) are estimated to be 1.3 and 2.4 nm. Assuming a proteinaceous pore, 6–7 and 10–11 helices, respectively, should be coassembled to allow the passage of these solutes (Sansom, 1991). Fattal et al. (1994) demonstrated that the melittin pore mediates a rapid flip-flop of the membrane lipids. If several lipid molecules are also involved in the pore lining, i.e., a peptide-lipid supramolecular complex constitutes the pore, as proposed for magainin 2 (Matsuzaki et al., 1996a) and mastoparan X (Matsuzaki et al., 1996b), the number of the helices involved will be smaller.

A similar phenomenon was also reported for melittin-induced hemolysis (Katsu et al., 1988). Pores of 1.3 and 2.4 nm are formed at melittin concentrations of $\sim$0.2 and 0.8 μM, respectively. The erythrocyte concentration used was 0.5% (v/v), corresponding to a lipid concentration of 20 μM. Therefore, the P/L values at which these pores are formed are 0.01 and 0.04, respectively, in keeping with Fig. 6.

The facts that melittin translocates across the bilayer and that its pore size depends on the P/L complicate interpretations of kinetic studies on pore formation: the pore formed first should have the largest size. The size subsequently becomes smaller upon translocation, because of a decrease in the peptide density on the outer monolayer.

CONCLUSION

In a series of studies, we have revealed that helical, pore-forming peptides magainin 2 (Matsuzaki et al., 1995a,b, 1996a), mastoparan X (Matsuzaki et al., 1996b), and melittin, possess very similar membrane-permeabilizing mechanisms, i.e., the pore formation-translocation mechanism. The pores appear to be composed of a dynamic, peptide-lipid supramolecular complex, allowing the mutually coupled transbilayer transport of ions, lipids, and peptides. These interactions are transient in nature, in that they are mainly observable during the early stage before equilibrium. The translocation phenomena can provide a molecular basis for the putative direct interactions of these peptides

with G-proteins on the cytoplasmic side (Hook et al., 1990; Mousli et al., 1990). Our findings indicate that the peptide-lipid interactions are more dynamic and complex than had been thought.

It should be noted that this class of peptides appears to differ from "genuine" pore formers, such as GALA (Parente et al., 1990). The latter peptides easily self-aggregate to form pores at extremely low P/L values of about 1/10,000. In contrast, the former needs much higher P/L values on the order of 1/100. If its pore formation is a consequence of relief of the expanded monolayer induced by the surface-lying monomer (He et al., 1996a), in other words, a "passive pore formation," one may then say that the membrane perturbation impairs the barrier property of the membrane. However, the typical channel former, alamethicin, also needs a high P/L value of 1/75 to induce the leakage of sucrose and KCl in the absence of the voltage (Portlock et al., 1990). Furthermore, no evidence for its aggregation was found (Archer et al., 1991). Taking into consideration the recent reports on the direct detection of pore structures of alamethicin (a helix bundle type) and magainin (a torus type) in the absence of the potential (He et al., 1996b; Ludtke et al., 1996), we conclude that amphiphilic helices potentially form pores of various structures and sizes, although interhelix interactions vary widely from peptide to peptide (from active aggregation to passive one). The application of the transmembrane potential modulates the pore formation process, including the pore structure. The physicochemical properties of the bilayer, such as fluidity and intrinsic curvature, are also regulators of pore formation.

The authors are indebted to Mr. Ken-ya Akada for his experimental assistance.

This work was supported by the Naito Foundation and Grants-in-Aid for Scientific Research on Priority Areas (08219223) and for Encouragement of Young Scientists (08772061) from the Ministry of Education, Science and Culture of Japan.

REFERENCES

Altenbach, C., and W. L. Hubbell. 1988. The aggregation state of spin-labelled melittin in solution and bound to phospholipid membranes: evidence that membrane-bound melittin is monomeric. *Proteins Struct. Funct. Genet.* 3:230–242.

Archer, S. J., J. F. Ellena, and D. S. Cafiso. 1991. Dynamics and aggregation of the peptide ion channel alamethicin. Measurements using spin-labeled peptides. *Biophys. J.* 60:389–398.

Bartlett, G. R. 1959. Phosphorus assay in column chromatography. *J. Biol. Chem.* 234:466–468.

Benachir, T., and M. Lafleur. 1995. Study of vesicle leakage induced by melittin. *Biochim. Biophys. Acta.* 1235:452–460.

Benachir, T., and M. Lafleur. 1996. Osmotic and pH transmembrane gradients control the lytic power of melittin. *Biophys. J.* 70:831–840.

Clague, M. J., and R. J. Cherry. 1989. A comparative study of band 3 aggregations in erythrocyte membranes by melittin and other cationic agents. *Biochim. Biophys. Acta.* 980:93–99.

Cornut, I., E. Thiaudiére, and J. Dufourcq. 1993. The amphipathic helix in cytotoxic peptides. *In* The Amphipathic Helix. R. M. Epand, editor. CRC Press, Boca Raton, FL. 173–220.

DeGrado, W. F., G. F. Musso, M. Lieber, E. T. Kaiser, and F. J. Kézdy. 1982. Kinetics and mechanism of hemolysis induced by melittin and by a synthetic melittin analogue. *Biophys. J.* 37:329–338.

Dempsey, C. E. 1990. The actions of melittin on membranes. *Biochim. Biophys. Acta.* 1031:143–161.

Dufourcq, J., J.-F. Faucon, G. Fourche, J.-L. Dasseux, M. LeMaire, and T. Gulik-Krzywicki. 1986. Morphological changes of phosphatidylcholine bilayers induced by mellitin: vesicularization, fusion, discoidal particles. *Biochim. Biophys. Acta.* 859:33–48.

Dufton, M. J., R. C. Hider, and R. J. Cherry. 1984. The influence of melittin on the rotation of band 3 protein in the human erythrocyte membrane. *Eur. Biophys. J.* 11:17–24.

Fattal, E., S. Nir, R. A. Parente, and F. C. Szoka, Jr. 1994. Pore-forming peptides induce rapid phospholipid flip-flop in membranes. *Biochemistry.* 33:6721–6731.

Fox, R. O., Jr., and F. M. Richards. 1982. A voltage-gated ion channel model inferred from the crystal structure of alamethicin at 1.5-Å resolution. *Nature.* 300:325–330.

Frey, S., and L. K. Tamm. 1991. Orientation of melittin in phospholipid bilayers. *Biophys. J.* 60:922–930.

He, K., S. J. Ludtke, W. T. Heller, and H. W. Huang. 1996a. Mechanism of alamethicin insertion into lipid bilayers. *Biophys. J.* 71:2669–2679.

He, K., S. J. Ludtke, D. L. Worcester, and H. W. Huang. 1996b. Neutron scattering in the plane of membranes: structure of alamethicin pores. *Biophys. J.* 70:2659–2666.

Hermetter, A., and J. R. Lakowicz. 1986. The aggregation state of melittin in lipid bilayers: an energy transfer study. *J. Biol. Chem.* 261: 8243–8248.

Hook, W. A., S. Tsuji, and R. Siraganian. 1990. Magainin-2 releases histamine from rat mast cells. *Proc. Soc. Exp. Biol. Med.* 193:50–55.

John, E., and F. Jänig. 1991. Aggregation state of melittin in lipid vesicle membranes. *Biophys. J.* 60:319–328.

Katsu, T., C. Ninomiya, M. Kuroko, H. Kobayashi, T. Hirota, and Y. Fujita. 1988. Action mechanism of amphipathic peptides gramicidin S and melittin on erythrocyte membrane. *Biochim. Biophys. Acta.* 939: 57–63.

Kempf, C., R. D. Klausner, J. N. Weinstein, J. V. Renswoude, M. Pincus, and R. Blumenthal. 1982. Voltage-dependent trans-bilayer orientation of melittin. *J. Biol. Chem.* 257:2469–2476.

Ludtke, S. J., K. He, W. T. Heller, T. A. Harroun, L. Yang, and H. W. Huang. 1996. Membrane pores induced by magainin. *Biochemistry* 35:13723–13728.

Matsuzaki, K. 1997. Membrane associated peptides. *In* Biomembrane Structures. D. Chapman and P. Haris, editors. IOS Press, Amsterdam. In press.

Matsuzaki, K., O. Murase, N. Fujii, and K. Miyajima. 1995a. Translocation of a channel-forming antimicrobial peptide, magainin 2, across lipid bilayers by forming a pore. *Biochemistry.* 34:6521–6526.

Matsuzaki, K., O. Murase, N. Fujii, and K. Miyajima. 1996a. An antimicrobial peptide, magainin 2, induced rapid flip-flop of phospholipids coupled with pore formation and peptide translocation. *Biochemistry.* 35:11361–11368.

Matsuzaki, K., O. Murase, and K. Miyajima. 1995b. Kinetics of pore formation induced by an antimicrobial peptide, magainin 2. *Biochemistry.* 34:12553–12559.

Matsuzaki, K., O. Murase, H. Tokuda, S. Funakoshi, N. Fujii, and K. Miyajima. 1994. Orientational and aggregational states of magainin 2 in phospholipid bilayers. *Biochemistry.* 33:3342–3349.

Matsuzaki, K., A. Nakamura, O. Murase, K. Sugishita, N. Fujii, and K. Miyajima. 1997. Modulation of magainin 2-lipid bilayer interactions by peptide charge. *Biochemistry.* 36:2104–2111.

Matsuzaki, K., S. Yoneyama, O. Murase, and K. Miyajima. 1996b. Transbilayer transport of ions and lipids coupled with mastoparan X translocation. *Biochemistry.* 35:8450–8456.

Mousli, M., J.-L. Bueb, C. Bronner, B. Rouot, and Y. Landry. 1990. G protein activation: a receptor-independent mode of action for cationic amphiphilic neuropeptides and venom peptides. *Trends Pharmacol. Sci.* 11:358–362.

Okada, A., K. Wakamatsu, T. Miyazawa, and T. Higashijima. 1994. Vesicle-bound conformation of melittin: transferred nuclear overhauser

enhancement analysis in the presence of perdeuterated phosphatidylcholine vesicles. *Biochemistry.* 33:9438–9446.

Parente, R. A., S. Nir, and J. F. C. Szoka. 1990. Mechanism of leakage of phospholipid vesicle contents induced by the peptide GALA. *Biochemistry.* 29:8720–8727.

Pawlak, M., S. Stankowski, and G. Schwarz. 1991. Melittin induced voltage-dependent conductance in DOPC lipid bilayers. *Biochim. Biophys. Acta.* 1062:94–102.

Portlock, S. H., M. J. Clague, and R. J. Cherry. 1990. Leakage of internal markers from erythrocytes and lipid vesicles induced by melittin, gramicidin S, and alamethicin: a comparative study. *Biochim. Biophys. Acta.* 1030:1–10.

Rink, T. J., and S. B. Hladky. 1982. Measurement of red cell membrane potential with fluorescent dyes. *In* Red Cell Membranes—A Methodological Approach. J. C. Ellory and J. D. Young, editors. Academic Press, London. 321–334.

Saberwal, G., and R. Nagaraj. 1994. Cell-lytic and antibacterial peptides that act by perturbing the barrier function of membranes: facets of their conformational features, structure-function correlations and membrane-perturbing abilities. *Biochim. Biophys. Acta.* 1197:109–131.

Sansom, M. S. P. 1991. The biophysics of peptide models of ion channels. *Prog. Biophys. Mol. Biol.* 55:139–235.

Schwarz, G., and A. Arbuzova. 1995. Pore kinetics reflected in the dequenching of a lipid vesicles entrapped fluorescence dye. *Biochim. Biophys. Acta.* 1239:51–57.

Schwarz, G., and G. Beschiaschvili. 1989. Thermodynamic and kinetic studies on the association of melittin with a phospholipid bilayer. *Biochim. Biophys. Acta.* 979:82–90.

Schwarz, G., and C. H. Robert. 1992. Kinetics of pore-mediated release of marker molecules from liposomes or cells. *Biophys. Chem.* 42:291–296.

Schwarz, G., R. Zong, and T. Popescu. 1992. Kinetics of melittin induced pore formation in the membrane of lipid vesicles. *Biochim. Biophys. Acta.* 1110:92–104.

Stankowski, S., M. Pawlak, E. Kaisheva, C. H. Robert, and G. Schwarz. 1991. A combined study of aggregation, membrane affinity and pore activity of natural and modified melittin. *Biochim. Biophys. Acta.* 1069: 77–86.

Steiner, H., D. Hultmark, Engström, H. Bennich, and H. G. Boman. 1981. Sequence and specificity of two antibacterial proteins involved in insect immunity. *Nature.* 292:246–248.

Terwilliger, T. C., L. Weissman, and D. Eisenberg. 1982. The structure of melittin in the form I crystals and its implication for mellitin's lytic and surface activities. *Biophys. J.* 37:353–361.

Tosteson, M. T., O. Alvarez, W. Hubbel, R. M. Bieganski, C. Attenbach, L. H. Caporales, J. J. Levy, R. F. Nutt, M. Rosenblatt, and D. C. Tosteson. 1990. Primary structure of peptides and ion channels: role of amino acid side chains in voltage gating of melittin channels. *Biophys. J.* 58:1367–1375.

Vogel, H. 1987. Comparison of the conformation and orientation of alamethicin and melittin in lipid membranes. *Biochemistry.* 26:4562–4572.

Weinstein, J. N., E. Ralston, L. D. Leserman, R. D. Klausner, P. Dragsten, P. Henkart, and R. Blumenthal. 1984. Self-quenching of carboxyfluorescein fluorescence: uses in studying liposome stability and liposome-cell interaction. *In* Liposome Technology. G. Gregoriadis, editor. CRC Press, Boca Raton, FL. 183–204.